Springer

KSME

Journal of Mechanical Science and Technology 30 (4) (2016) 1691~1704
www.springerlink.com/content/1738-494x(Print)/1976-3824(Online)
DOI 10.1007/s12206-016-0325-0

Variation of wake patterns and force coefficients of the flow past square bodies aligned inline †

Raheela Manzoor[1], Shams-ul-Islam[1,*], Waqas Sarwar Abbasi[1] and Sajida Parveen[2]

[1]*Mathematics Department, COMSATS Institute of Information Technology, Islamabad 44000, Pakistan*
[2]*Mathematics Department, Sardar Bahadur Khan Women University, Quetta 87300, Pakistan*

(Manuscript Received November 2, 2015; Revised December 10, 2015; Accepted December 14, 2015)

Abstract

In this numerical study, the variation of wake patterns and force coefficients of the flow past four square bodies aligned inline are investigated. A two-dimensional numerical code is developed using the Lattice Boltzmann method (LBM) for this study. The code is first validated for the flow past a single and two tandem square cylinders. The results are compared to those available in literature and found to be in good agreement. After validation the calculations are further performed to investigate the effect of gap spacing (g) for the flow past four inline square cylinders at two different Reynolds numbers (Re) 100 and 200. The gap spacing is chosen in the range $0.25 \leq g \leq 7$. Six different flow patterns: Single slender body, alternate reattachment, quasi steady reattachment, intermittent shedding, chaotic flow and periodic flow are found in this study with successive increment in spacing. It is found that some flow patterns existing at Re = 100 do not exist at Re = 200. The generated vortices at Re = 200 are much stronger as compared to those at Re = 100. The spacing value g = 3 is found to be critical at Re = 100 while at Re = 200 the spacing value g = 2 is critical due to abrupt changes in flow characteristics. At some spacing values the downstream cylinders have higher values of average drag coefficients as compared to upstream ones. In general the upstream cylinder (c1) have higher drag forces at Re = 200 than at Re = 100. The root mean square values of lift coefficient are found to be greater than the corresponding root mean square values of drag coefficient.

Keywords: Flow patterns; Force coefficients; Gap spacing; Inline square cylinders; Lattice Boltzmann method

1. Introduction

Flows around multiple structures are mostly seen in engineering problems. Examples of such problems can be found in high rise buildings, bridges, cooling towers, chimneys and electronic equipments etc. Such types of structures often interact with steady or unsteady fluid flows and experience flow induced forces like drag and lift. In case of unsteady flows the vortices shed alternately from the two sides of a structure. Structural oscillations occur as a result of alternate vortex shedding, which may affect the wake structure mechanism and impact upon fluid dynamics around downstream structures. It is of both practical and fundamental importance to experimentally and numerically study the possible influences of the upstream structure effects on the downstream flow. In such cases the cylinders are either in tandem, side-by-side or staggered arrangements. Flow around cylindrical bodies is affected by many parameters such as Reynolds numbers ($Re = U_\infty d/\upsilon$; where U_∞ is the uniform inflow velocity, d is the size of body and υ is the kinematic viscosity), shape and size of the bodies and surface roughness [1]. Most of the researchers have worked on the flow past a single cylindrical body (Square/circular) both numerically as well as experimentally (Shih et al. [2], Niemann and Holscher [3], Manzoor et al. [4], Franke et al. [5] and Saha et al. [6]). Shih et al. [2] performed experiments on flow past circular cylinders at large Re with different surface roughness values. They concluded that at sufficiently large Re values the drag coefficient of cylinder does not depend on Re but it depends on the roughness of surface of the cylinder. Also the roughest cylinder have lowest Strouhal number ($St = f_s d/U_\infty$; where f_s is the vortex shedding frequency) value. Niemann and Holscher [3] termed circular cylinders as semi aerodynamic bodies. According to them, these semi aerodynamic bodies differ from other bodies (Airfoils and square shaped) due to separation point of the flow. The separation of flow from these bodies depends on different parameters such as free-stream velocity, flow profile, free-stream turbulence, geometry and surface roughness. Manzoor et al. [4] experimentally measured the vortex-induced vibrations of a square cylinder in a wind tunnel. They found that no significant oscillations of square cylinder were seen at lower mean free stream velocity $U_r < 6$. But at $U_r \approx 10$ and 14 the vortex shedding frequency and the natural frequency of the

*Corresponding author. Tel.: +92 3139840066
E-mail address: islam_shams@comsats.edu.pk
† Recommended by Associate Editor Mofreh Ghabour

cylinder matched exactly. The authors termed this value of U_r as critical flow velocity. Franke et al. [5] performed numerical calculations for the flow past single circular and square cylinder. They reported that up to Re = 1000 and 300 flow remains fully laminar for the circular and square cylinders, respectively. Beyond these Re values the turbulent model is necessary to describe the flow characteristics. According to Saha et al. [6] flow past a square cylinder remains in steady state up to Re = 40 and becomes chaotic around the value Re = 600. Between these two states it under goes a sequence of transitions by changing Re values. Further work on the flow past single cylindrical body can be cited in Refs. [7-10].

In case of more than one body in the flow field a very important influencing parameter, gap spacing (g), comes into play. This parameter is more effective than Re in terms of flow characteristics. Some representative papers for flow past two tandem cylinders will be discussed in this section. The effect of g, for the flow past two tandem cylindrical bodies, along with other influencing parameters has been studied extensively by most of the researchers [11-20]. Xu and Zhou [11] experimentally measured the Strouhal numbers in the wake of two tandem circular cylinders in the range of Re = 800 to 4.2×10^4 and g = 1 to 15. They observed that the spacing range g = 3.5 to 5 is critical. Below this range the St behind the downstream cylinder drops rapidly by increasing g due to the fact that vortices do not shed between the gaps while for spacing values above the critical range co-shedding occurs which results increase in the values of St with g. Kim et al. [12] performed experiments to measure the flow fields around two square cylinders in tandem arrangement in the spacing range g = 0.5 to 10 at Re = 5300 and 16000. They reported that the flow patterns for $g \leq 2$ were quite different from those at $g \geq 2.5$ due to reattachment of shear layers separated from upstream cylinder. The authors termed g = 2.5 as critical value of spacing and categorized the flow characteristics in two modes separated by the critical value. Lankadasu and Vengadesan [13] numerically studied the effect of g and shear parameter (K) on the flow past two tandem square cylinders at Re = 100 and concluded that at lower values of g and K the downstream cylinder have negative values of mean drag coefficient (Cdmean). Also at K = 0 and 1 the flow showed steady behavior till g = 4 and 3 respectively and it becomes unsteady at early stages (smaller values of g) by increasing the value of K. For $g < 4$ vortices shed only behind the downstream cylinder but for $g > 4$ both the cylinders start shedding vortices. Sohankar [14] divided the flow past two tandem square cylinders into three regimes depending on g. (i) Single slender-body regime ($g < 0.5$), (ii) the reattach regime ($g < 4$) and (iii) the co-shedding or binary vortex regime ($g \geq 4$). The author also concluded that at Re = 200 the three dimensional effects start appearing in the flow characteristics. Patil and Tiwari [15] performed numerical simulations in order to study the effect of relative cylinder sizes, g and Re on the flow around two square cylinders in tandem arrangement. They observed that for relative cylinder size greater than one the vortex shedding from the downstream cylinder vanishes. The drag coefficient ($Cd = 2F_d/\rho U^2_\infty d$; where F_d is drag force, ρ is the density of fluid) of the upstream cylinder remains positive and increases with relative cylinder size values while that of downstream cylinder is negative and decreases by increasing the value of relative cylinder size. For the spacing value $g < 2$ vortices do not shed behind any of the cylinder while at g = 5 the vortices start shedding from both the cylinders. Flows past tandem circular and square cylinders for some important engineering parameters are discussed in detail elsewhere [16-20].

With the addition of two or more cylinders in the wake of a single cylinder the fluid forces and wake patterns are quite different as compared to those in the case of a single or two tandem cylinders due to the fact that there are more than one gap spacing. This phenomenon is also studied by many researchers. Igarashi and Suzuki [21] performed experimental investigations on the characteristics of flow around three circular cylinders aligned inline and divided the behavior of shear layers in three cases. (i) Without reattachment, (ii) with reattachment and (iii) rolling up. They observed that the Cd of the middle cylinder is negative for the spacing values $g < 3.53$ while that of the downstream cylinder remains positive. This phenomenon is different from two cylinders case in which the downstream cylinder has negative value of Cd. Harichandan and Roy [22] numerically investigated the flow around three inline circular cylinders at Re = 100 and 200 at different spacing values. They deduced that the downstream cylinder experiences very large unsteady forces which can give rise to wake-induced flutter. This phenomenon is more likely to occur at small values of g. At Re = 100 and g = 2 they observed steady wake pattern while sparse Karman street was seen at Re = 200 and g = 2. At g = 5 the Karman vortex streets were observed between the cylinders at both Re values. Vasel-Be-Hagh et al. [23] studied the effects of Re on the force coefficients of the air flow past three circular cylinders aligned inline at g = 2. They found that the time averaged lift force remains zero for all the cylinders over the studied conditions. The pressure and viscous drag forces decrease while St increases with increasing Re values. The flow became unsteady at $Re \geq 101$while at Re = 105 the shedding of vortices started. Islam et al. [24] divided the flow around three inline square cylinders into five different wake modes: steady wake, nearly unsteady wake, sparse Karman vortex street, non-fully developed vortex street in single row and double row, with respect to spacing. They found a critical value of spacing at g = 3 due to abrupt changes in the flow characteristics. Bao et al. [25] numerically simulated the flow around six inline square cylinders in the spacing range $1.5 \leq g \leq 15$ at Re = 100 and categorized the flow into six different patterns: Steady wake, non-fully developed vortex street in single row and double row, fully developed vortex street in double row, fully developed vortex street in partially recovered single row and fully developed multiple vortex streets. They further reported that the flow mode changes from steady to unsteady state as the spacing crosses a critical value. Sewatkar et al. [26] studied the

flow around six inline square cylinders numerically as well as experimentally at $0.5 \le g \le 10$ and $80 \le Re \le 320$. At Re = 100 they observed synchronous flow regime in the spacing range $0.5 \le g \le 1.1$, quasi-periodic-I regime at $1.2 \le g \le 1.3$, quasi-periodic-II regime at $1.4 \le g \le 5$ and chaotic flow in the spacing range $6 \le g \le 10$. They concluded that the quasi periodic and chaotic nature of the flow is due to the wake interference of the upstream cylinders and it becomes more severe at higher Re values. It is important to mention here that for inline (Tandem) structures the effect of drag force is more important compared to lift forces because the drag forces either push these bodies in the direction of flow or may pull the structures in opposite direction due to thrust. There have been a lot of work in order to reduce the drag forces on the structures by placing small control cylinders or splitter plates in the flow filed.

From above discussion it can be deduced that much less attention has been given to the studies for flow past more than two bodies aligned inline. There is no such documentations on the effect of gap spacing for four tandem square cylinders for fixed Re to the best of our knowledge and on a best efforts basis. With these points in mind the present study focuses on: (i) The effects of spacing on the flow past four square cylinders aligned in-line at fixed Re (ii) changes in these effects by changing Re (ii) variation of wake patterns and force statistics with spacing (iii) applicability of lattice Boltzmann method for flow past such complex geometries. Also in this work a special emphasis is given on the effect of addition of cylinders in inline arrangement and spacing between these cylinders on drag forces. In the following sections these points will be analyzed in detail.

2. Lattice Boltzmann method

In this section the LBM is briefly introduced. The Lattice Boltzmann method (LBM) is an effective alternative numerical technique as compared to traditional Computational fluid dynamics (CFD) with some advantages, such as the natural parallelism and ease to handle interaction between fluids or phases [27]. LBM is a particle based method and it uses different models. In this paper we will use a two-dimensional and nine velocity particles (*D2Q9*, where *D* is dimension and *Q* is the number of particles) model. In LBM, at each time step the pressure is determined from the equation of state ($P = \rho c_s^2$, where ρ is the fluid density and $c_s = \sqrt{RT} = 1/\sqrt{3}$ is the speed of sound for *D2Q9* model) for ideal gases. The speed of sound does not depend on the temperature *T* or any other adjustable parameter in this method [28]. *R* is the gas constant. In LBM, it is not necessary to solve a Poisson equation for the pressure. Compared with common CFD methods this saves significant computer Central processing unit (CPU) time.

The workhorse of the LBM is the Boltzmann transport equation:

$$\partial f/\partial t + \partial f/\partial \boldsymbol{x}.\boldsymbol{e} + \boldsymbol{F}/m.\partial f/\partial \boldsymbol{e} = \Omega \quad (1)$$

where $f(\boldsymbol{x}, \boldsymbol{u}, t)$ is the particle distribution function, $(\boldsymbol{x}, \boldsymbol{e})$ is the phase space variable, t is the time, $\boldsymbol{F}$ is the external force (e.g., gravity) and Ω is the collision operator. In this study we use the LBM without external forces ($\boldsymbol{F} = 0$).

Using the Grad expansions or Chapman-Enskog [29] it can be proved that the equation is consistent with the Navier-Stokes equations in the hydrodynamic limit. Particle velocity space can be reduced to a set of discrete velocities $\{\boldsymbol{e}_i | i = 1,\ldots,b\}$ and the construction of the lattice, on which the calculations are carried out. Usually the equation is approximated along characteristic velocity vectors:

$$f_i(\boldsymbol{x} + \boldsymbol{e}_i, t + 1) = f_i(\boldsymbol{x}, t) - 1/\tau[f_i(\boldsymbol{x}, t) - f_i^{(eq)}(\boldsymbol{x}, t)] \; \forall \; i = 0,1,\ldots,b \quad (2)$$

where $f_i(\boldsymbol{x}, t) \equiv f_i^{(eq)}(\rho, t)$ is the equilibrium distribution function of ith discrete velocity and τ is the single-relaxation-time parameter.

Numerically, Eq. (2) is solved in two steps:

Streaming:

$$f_i^{(in)}(\boldsymbol{x}, t) = f_i^{(out)}(\boldsymbol{x} - \boldsymbol{e}, t - 1). \quad (3)$$

Collision:

$$f_i^{(out)}(\boldsymbol{x}, t) = f_i^{(in)}(\boldsymbol{x}, t) - 1/\tau[f_i^{(in)}(\boldsymbol{x}, t) - f_i^{(eq)}(\boldsymbol{x}, t)]. \quad (4)$$

During streaming step Eq. (3) distribution functions are transferred to their neighbor lattice site according to their velocity vectors. The particle distribution functions approach their equilibrium distributions in the collision step Eq. (4). The incoming and outgoing distribution functions, i.e., before and after collision, are denoted with "in" and "out" indices respectively. The macroscopic density ρ and momentum $\rho\boldsymbol{v}$ in a cell are the 0th and 1st moments of the distribution functions:

$$\rho = \sum_{i=0}^{b} f_i, \quad \rho \boldsymbol{v} = \sum_{i=0}^{b} f_i \boldsymbol{e}_i \,. \quad (5)$$

In terms of discrete velocities $\boldsymbol{e}_i$ the equilibrium distribution functions are defined as

$$f_i^{(eq)}(\boldsymbol{x}, t) = w_i \rho[1 + 3(\boldsymbol{e}_i.\boldsymbol{u})/c^2 + 4.5(\boldsymbol{e}_i.\boldsymbol{u})^2/c^4 - 1.5\boldsymbol{u}^2/c^2] \,. \quad (6)$$

The weighting coefficients (w_i) which are the constants for the nine-velocity two-dimensional model are

$$w_0 = 4/9, \quad (7a)$$

$$w_1 = w_2 = w_3 = w_4 = 1/9, \quad (7b)$$

$$w_5 = w_6 = w_7 = w_8 = 1/36. \quad (7c)$$

The *D2Q9* lattice structure is given in Fig. 1.

The viscosity is defined from: $\upsilon = 1/3(\tau - 0.5)$.

3. Geometry and boundary conditions

The schematic diagram for flow past four inline square cylinders of same size 'd' is presented in Fig. 2. Cylinder c1 is

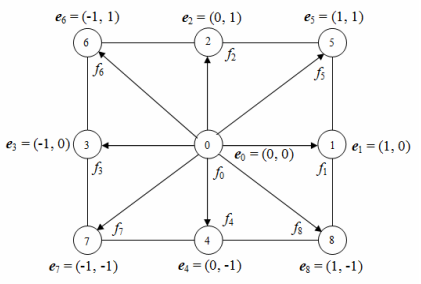

Fig. 1. *D2Q9* particles direction.

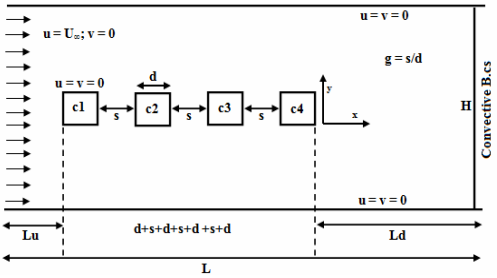

Fig. 2. Schematic diagram for the flow past four in-line square cylinders.

the upstream cylinder placed at a position Lu = 6d from the inlet position while cylinder c4 is downstream cylinder at the position Ld = 25d from the outlet position. The other two cylinders c2 and c3 are placed between these two cylinders. Surface to surface distance between the cylinders is denoted by s while the gap spacing (g = s/d) between cylinders is normalized using the surface to surface distance and size of the cylinder. The computational domain has a fixed height H = 11d. The length (L) of computational domain varies by varying gap spacing (see Table 1).

At the inlet position a uniform inflow condition (**u** = U_∞**; v** = 0**)** is used, where U_∞ is inflow velocity along the horizontal direction while **v** = 0 indicates that there is no flow in vertical direction. The convective boundary condition (∂_t**u** + $U_\infty\partial_x$**u** = 0) is used at the outlet position of the channel [30]. At the surface of cylinders no-slip condition (**u** = **v** = 0**)** is used. In LBM the no-slip condition is applied using the bounce back treatment in which the particles hitting the solid wall return back to their previous position. The no-slip condition is also applied at upper and lower walls of the channel. This is one of the advantages of the LBM that no-slip boundary condition can be easily handled by simple bounce-back scheme. In our study, in the computational domain any lattice node represents either a fluid node or a solid node. To use the no-slip wall boundary conditions it is important to implement the bounce-back algorithm instead of the collision step before the streaming step. The total fluid force on the square cylinder is calculated using the momentum exchange method [31]. It is observed that the present LBM study using U_∞ = 0.04385964 give reasonably good results for τ = 0.526315784 and 0.513157892 for Re = 100 and 200, respectively, and d = 20. The code for this problem was originally written and edited using Compaq visual fortran version 6.5.0.

4. Code validation and grid independence study

For spatial adequacy the present code was tested by varying the number of grid points (10, 20 and 40 points) along the surface of the cylinder. The resulting Cdmean, St and Clrms were compared at Re = 100 and 200 (Table 2). For the 10-points grid, the computational domain comprises 320 and 110 points along the longitudinal and transverse directions, respectively. The cylinder is placed 6d from inlet and 25d from the outlet position. It can be observed from the table that the computations on the 20-points grid gives better results in terms of computational time and convergence. Guo et al. [30] also suggested that 20-points grid is enough for convergence.

In order to choose a suitable computational domain for better accuracy and computational time, we have calculated the values of Cdmean and St for the flow past two in-line square cylinders at different values of inlet, outlet and height of the computational domain. A comparison of these values is presented in Table 3. It can be seen from the table that by fixing Ld and H at 25d and 11d, respectively, the Cdmean and St of both the cylinders decreases with increment in the upstream distance (Lu). That's why we have chosen the upstream length Lu = 6d in our study. Although Lu = 8d gives better results but it takes more computational time as compared to Lu = 6d because it uses more number of grid points. The upstream distance has a great influence on the generation of vortices. The shedding of vortices starts as quicker as a cylinder is placed nearer to the inlet position. Due to this fact the smaller value Lu = 4d is not taken because it can affect the physical parameters. Also it will be seen the later paragraphs that at this value of Lu the values of physical parameters agrees well those of other researchers. Similarly by fixing Lu at 6d and changing the values of Ld and H, it can be seen that Ld = 25d and H = 11d gives better results than other chosen values. So we have selected Lu = 6d, Ld = 25d and H = 11d in our study to ensure better accuracy and less computational time. Also these values agree well with those of other researchers [5, 6, 13, 15].

In order to validate our study we have calculated the values of different fluid forces like Cdmean, St, Cdrms and Clrms for flow past a single square cylinder at Re = 100 and 200. The numerical method was validated compared the results obtained by other numerical techniques for the flow around a single square cylinder (see Table 4). It can be observed that the present data shows a good agreement with the experimental as well as numerical values. This indicates that the present code can simulate the flow characteristics in an efficient manner.

To study the effect of addition of bodies in stream wise direction, on the force coefficients, we have calculated the Cdmean of first cylinder for flow past two inline, three inline, four inline and five inline cylinders. A comparison of these

Table 1. Selected cases for current study at Re = 100 and 200.

Cases	L × H	Cases	L × H
g = 0.25	716 × 221	g = 3	881 × 221
g = 0.5	731 × 221	g = 3.5	911 × 221
g = .75	746 × 221	g = 4	941 × 221
g = 1	761 × 221	g = 5	1001 × 221
g = 1.5	791 × 221	g = 6	1061 × 221
g = 2	821 × 221	g = 7	1121 × 221
g = 2.5	851 × 221		

Table 2. Effect of spatial resolution on the physical parameters of the flow past a single square cylinder at Re = 100 and 200.

	10-points	20-points	40-points
Cdmean (Re = 100)	1.4630 (1.34%)	1.4434 (0.2%)	1.4414
St (Re = 100)	0.1498 (0.5%)	0.1491 (0%)	0.1491
Clrms (Re = 100)	0.1798 (3.1%)	0.1742 (1.2%)	0.1762
Cdmean (Re = 200)	1.5214 (0.1%)	1.5198 (0.8%)	1.5086
St (Re = 200)	0.1518 (2%)	0.1549 (0%)	0.1549
Clrms (Re = 200)	0.4496 (0.8%)	0.4534 (0.09%)	0.4538

Table 3. Domain independence study at Re = 100 and g = 5.

Case	Cdmean1	Cdmean2	St1	St2
Lu = 4d; Ld = 25d; H = 11d	1.501	1.394	0.148	0.148
Lu = 6d; Ld = 25d; H = 11d	1.432	1.303	0.143	0.143
Lu = 8d; Ld = 25d; H = 11d	1.412	1.277	0.142	0.142
Lu = 6d; Ld = 20d; H = 11d	1.432	1.302	0.143	0.143
Lu = 6d; Ld = 30d; H = 11d	1.432	1.303	0.143	0.143
Lu = 6d; Ld = 25d; H = 9d	1.476	1.377	0.148	0.148
Lu = 6d; Ld = 25d; H = 13d	1.408	1.255	0.141	0.141

values with Single cylinder (SC) values with percentage reduction is presented in Table 5. It can be seen that the percentage reduction in Cdmean of c1 increases with the addition of bodies in stream wise direction. Because the Cdmean of c1, for four and five inline cylinders, has highest percentage reduction (8.02%). In case of four and five in-line cylinders the drag reduction in percentage is same. From here it can be inferred that more the number of bodies in inline arrangement lesser will be the value of Cdmean of first cylinder. It indicates that the addition of bodies in stream wise direction affects the flow characteristics significantly. On the basis of above analysis we choose four cylinders in inline arrangement for current numerical investigation. The selected cases, at Re = 100 and 200, for the current study are presented in Table 1.

Here, firstly, some silent features and issues will be presented. Numerically researchers either interested in confined (Blockage) and unconfined (without blockage) effect to investigate the flow past a bluff body inside the channel. In case of blockage the boundary layers also plays an important role and affect the wake structure mechanism and force statistics as

Table 4. Comparison of Cdmean, St, Cdrms and Clrms for flow past a single square cylinder at Re = 100 and 200.

	Cdmean		St	
Re	100	200	100	200
Saha et al. [6]	1.510	1.670	0.159	0.163
Sohankar et al. [9]	1.444	1.424	0.145	0.165
Okajima [32]	1.600	1.480	0.141	0.138
Norberg [33]	…	1.450	0.140	0.152
Abograis and Alshayji [34]	1.480	1.488	0.140	0.153
Present	1.443	1.519	0.149	0.155
	Cdrms		Clrms	
Re	100	200	100	200
Sohankar et al. [9]	0.002	0.012	0.130	0.240
Abograis and Alshayji [34]	0.006	0.027	0.158	0.332
Present	0.006	0.038	0.174	0.453

Table 5. Percentage reduction in Cdmean of first cylinder (c1) with addition of cylinders in in-line arrangement at Re = 100 and g = 2.

	Single cylinder	Two inline	Three inline	Four inline	Five inline
Cdmean	1.444	1.338	1.329	1.328	1.328
% reduction	---	7.3	7.9	8.02	8.02

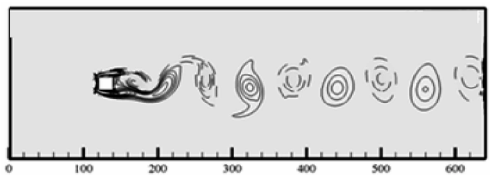

(a)

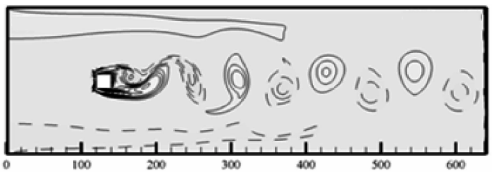

(b)

Fig. 3. Vorticity contours visualization of flow past single square cylinder: (a) Unconfined flow; (b) confined flow.

compared to unconfined flows. In case of unconfined we need to have reasonably good height of the computational domain to diminish the wall effect on flow past bluff body. One can clearly see such differences in Figs. 3(a) and (b) for flow past a single square cylinder at Re = 100. In case of blockage β = H/d = 8d and in unconfined case H = 11d. It should be noted that the vorticity is detected in the flow field using the following relation

$$\nabla \times \mathbf{u} = \partial v/\partial x - \partial u/\partial y \,. \quad (8)$$

For convergence normally two different approaches are used. Firstly, calculations are terminated once the temporal

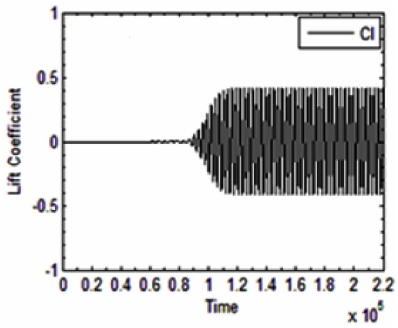

Fig. 4. Time-trace analysis of lift coefficient for flow past a single square cylinder at Re = 200.

variation of the lift coefficient becomes periodic (see Fig. 4). Secondly, one can stop the numerical calculation once the below criteria is satisfied.

$$\text{Error} = \frac{\sqrt{\sum_{i,j}\left[u_{i,j}(c+1)-u_{i,j}(c)\right]^2}}{\sqrt{\sum_{i,j}\left[u_{i,j}(c+1)\right]^2}} \leq 5\times 10^{-8}\,. \tag{9}$$

When the temporal variation of the lift force becomes periodic, the calculations will be terminated. In case of multiple bodies, it is almost difficult to adopt this procedure until all the cylinders lift forces becomes periodic. In such situation we use Eq. (9) for calculations termination. Interesting readers can also read research papers related to fluid-structure interaction problems, lattice Boltzmann method and flow transitions for bluff bodies [35-41].

5. Results and discussions

5.1 Wake patterns

In this section a detailed analysis of different flow patterns, revealed in this study, is presented in terms of vorticity contours, temporal histories of drag and lift coefficients, and stream lines. Different flow patterns reported in the literature for inline cylinders are single slender body, alternate reattachment, quasi steady reattachment, intermittent shedding, chaotic flow and binary vortex street ([1, 26]). These flow patterns were again identified in the current study for flow past four square cylinders aligned inline but within different range of spacing and in modified form. In the following subsections these flow patterns are discussed in detail. The solid lines in the vorticity contours represent positive vortices emerging from lower corners of cylinders and moving anticlockwise. While the dashed lines represent negative vortices emerging from upper corners and moving clockwise. For the sake of brevity only those figures are presented which show different behavior of flow. Similar figures are not presented to reduce length of paper.

5.1.1 Single slender body (SSB)

The vorticity contours for the case g = 0.25 and Re = 100, 200 are shown in Figs. 5(a) and (b). It can be seen that due to narrow space there is no flow interaction in the gaps between the cylinders and the shear layers emerging from the upstream side of c1 form vortices at downstream position of c4 only. This can also be observed from streamlines representation (Fig. 19(a)). All the cylinders behave like an isolated body in the flow field. Zdravkovich [1] classified this flow behavior as Single slender body (SSB) which exists in the spacing range 1 ≤ g ≤ 1.8 for two tandem circular cylinders. This type of flow is also termed as 'single bluff body' in the Ref. [26]. It can also be observed that at Re = 100 sparse vortices are formed as compared to those at Re = 200. Also the vortex rollup point moves further upstream at Re = 200 as compared to that at Re = 100. Similar flow characteristics were observed at (Re, g) = (100, 0.5) and (Re, g) = (200, 0.5) (Figures not shown).

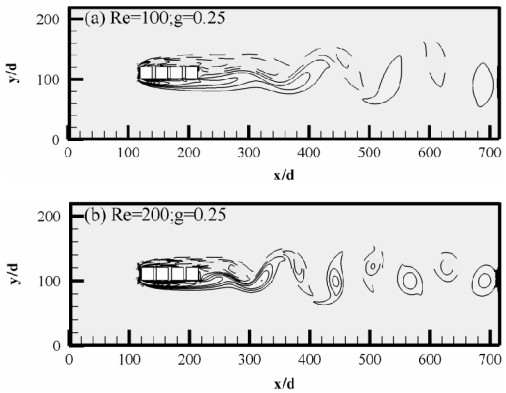

Fig. 5. Vorticity contours visualization for SSB flow.

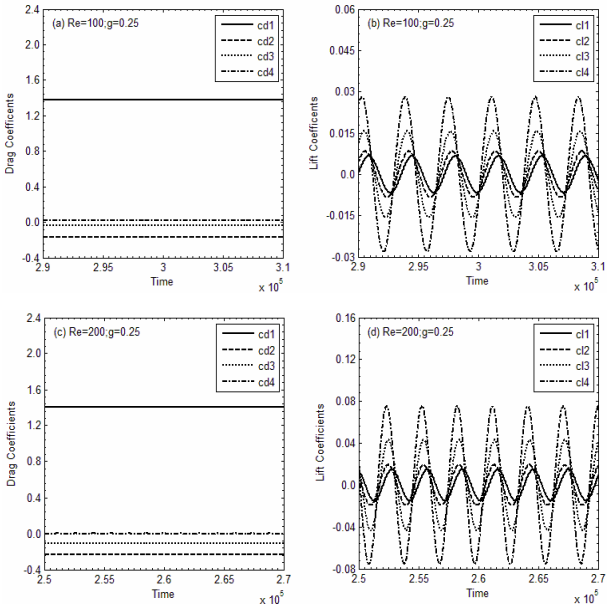

Fig. 6. Temporal histories of drag and lift coefficients for SSB flow.

The temporal histories of drag coefficients confirm that there is no flow interaction between the gaps and constant drag forces are exerted by the flow on cylinders (Figs. 6(a)

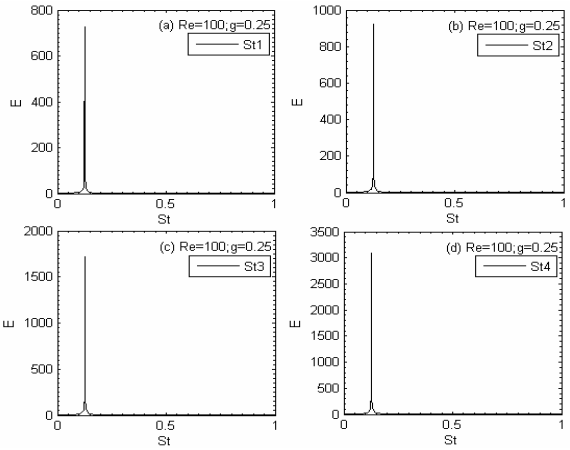

Fig. 7. Power spectrum analysis of lift coefficients for SSB flow.

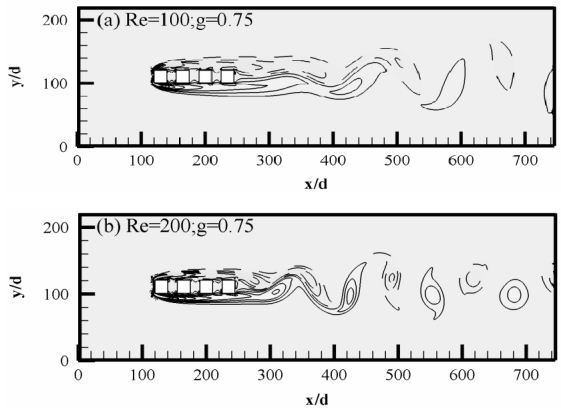

Fig. 8. Vorticity contours snapshots for AR flow.

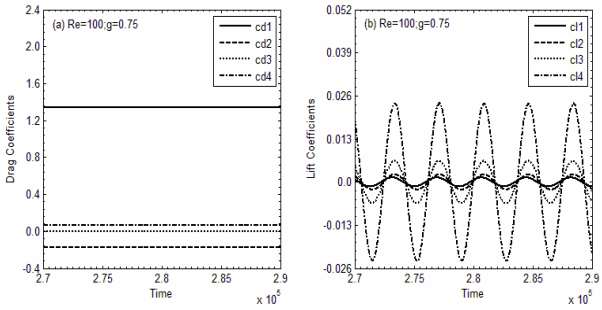

Fig. 9. Variation of drag and lift coefficients with time for AR flow.

and (c)). It can be observed that the drag coefficients of c2 and c3 are negative. This is due to the fact that the spacing between the cylinders is narrow and a strong suction is created in the gaps due to this narrow space. As a result the drag forces become negative and act in the opposite direction of flow. Due to this phenomenon c2 and c3 are pulled upstream instead of being pushed downstream. While the lift coefficients have periodic behavior with the last cylinder having largest amplitude which indicates the generation of vortices at downstream position (Figs. 6(b) and (d)). It can also be seen that the relative amplitudes of lift coefficients of cylinders at Re = 100 are less than those at Re = 200. Which is due to the fact that with the increment in Re the viscous forces become weaker. As a result strengthen vortices shed from cylinders. Due to these strengthen vortices the amplitude of lift cycles increases.

The power spectrum of lift coefficients for SSB flow is shown in Figs. 7(a)-(d). A single peak in the power spectra graphs indicates the dominancy of a single frequency which is vortex shedding frequency for all the cylinders. According to Sewatkar [26] the sinusoidal nature of lift coefficient indicates a single frequency in the power spectrum analysis. Further it can be seen that spectrum energy of the consecutive cylinders is increasing, that is, the first cylinder (c1) have lowest spectrum energy while the last cylinder (c4) has largest spectrum energy. This shows that larger the amplitude of lift cycles higher will be the spectrum energy (Figs. 6(b) and 7(a)-(d)). Similar characteristics were observed at (Re, g) = (200, 0.25) (Figures not shown).

5.1.2 Alternate reattachment (AR)

With the slight increment in the spacing the flow is no more SSB (see Fig. 8(a)). It can be observed that the inner shear layers emerging from c1 reattach to c2, then to c3 and c4. This flow pattern is categorized as Alternate reattachment (AR). The shear layers are slightly suppressed inside the gaps between the cylinders due to the increment in spacing. Like SSB flow case the strengthen vortices can be seen at Re = 200 (Fig. 8(b)). The alternate reattachment of shear layers can also be confirmed from the streamlines representation (Fig. 19(b)). The streamlines indicate that the flow moves from lower to upper corners of cylinders. Two stagnant recirculation zones are formed between each gap which indicates the formation of vortices at these points but due to small space these vortices diminish quickly before formation. Similar flow behavior was observed at Re = 100, g = 1 and 1.5 and at (Re, g) = (200, 1) (Figures not shown). Igarashi and Suzuki [21] named this type of behavior of shear layers as 'with reattachment and roll up' for flow past three circular cylinders while according to Zdravkovich [1] this flow occurs in the spacing range $1.2 < g < 3.4$ depending on Re for two tandem cylinders case.

The temporal variation of drag and lift coefficients for AR flow are shown in Fig. 9. The drag coefficients of all the cylinders are straight lines which indicate that vortices are not formed between the gaps. Unlike SSB flow case here only the drag coefficient of c2 is negative. The lift coefficients of all the cylinders are periodic indicating the single frequency (Vortex shedding frequency) in the power spectra analysis. Also it can be seen that the amplitudes of lift cycles of all the cylinders are smaller as compared to those in SSB flow (see Figs. 9(b) and 6(b)). This is due to the fact that in AR flow the wake circulation length also increases with increment in gap spacing, resulting in decrease in lift amplitudes. Because larger the wake circulation length smaller will be the amplitude of drag and lift coefficients. The power spectra graphs are not

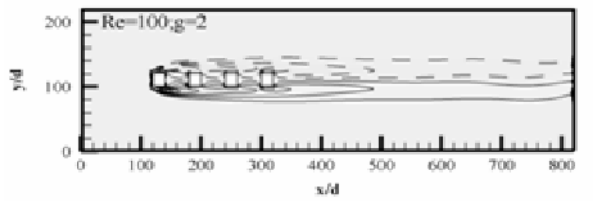

Fig. 10. Vorticity snapshots for QSR flow.

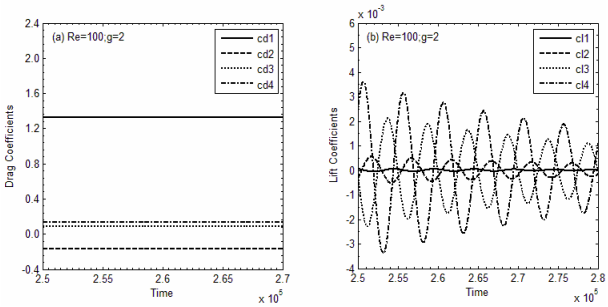

Fig. 11. Time variation of drag and lift coefficients for QSR flow.

shown here due to similarity with Fig. 7.

5.1.3 Quasi steady reattachment (QSR)

At (Re, g) = (100, 2) it can be seen that the shear layers roll up neither within the gaps nor at downstream position of c4 to form vortices. Initially the flow is steady, exhibiting some unsteadiness at the far downstream position but the vortices are not still formed. Also the flow from upper and lower sides of cylinders is symmetric about the centerline of cylinders. Due to increment in spacing the shear layers move further inside the gaps (Fig. 10). Due to this movement we observe wider stagnant recirculation zones between the cylinders in the streamlines representation (Fig. 19(c)). The initial steadiness of flow can be confirmed from the streamlines behaviour. Due to these characteristics this flow is named as Quasi steady reattachment (QSR). Like SSB and AR flow the drag coefficients show constant behavior while the lift coefficients have periodic behavior with decaying amplitude of consecutive cycles (Fig. 11). This is due to the fact that with the passage of time the viscosity stabilizes the flow by reducing the unsteadiness produced in the flow. Similar behavior of lift coefficients was reported by Ghadiri et al. [17] at (Re, g) = (100, 2.5) for two tandem circular cylinders. It should be noted that this type of flow behavior was not observed at all the chosen gap spacings at Re = 200. In the power spectra analysis only the primary frequency was dominant and the role of secondary frequency (Cylinder interaction frequency) was negligible (Figure not shown).

5.1.4 Intermittent shedding (IS)

The Intermittent shedding (IS) flow pattern was observed at (Re, g) = (100, 2.5) and (Re, g) = (200, 1.5) (Fig. 12). In this pattern the shear layers that detach from c1 show asymmetric reattachment at the downstream cylinders. As it can be seen that, from upper sides of cylinders, the outer shear layers first

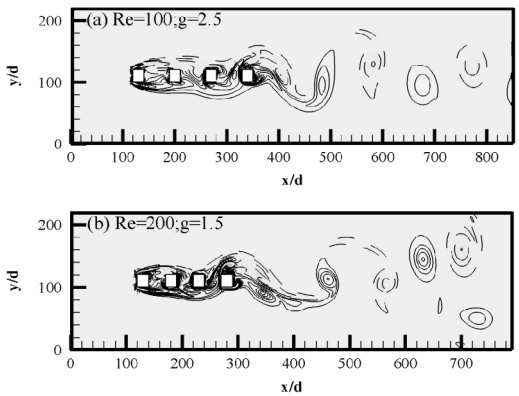

Fig. 12. Vorticity contours for IS flow.

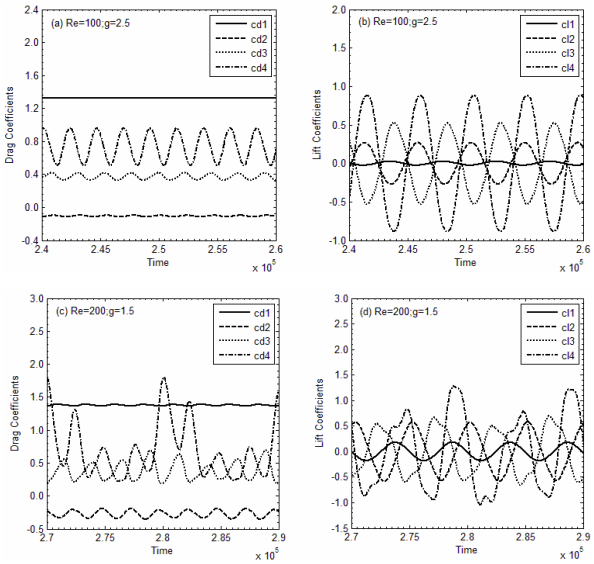

Fig. 13. Temporal variation of drag and lift coefficients for IS flow.

reattach to the third cylinder (c3). Then after detaching from c3 these shear layers roll up to form vortices at downstream position of c4 while the inner shear layers reattach to c4. From lower sides of cylinders, the outer shear layers after detaching from c1 first reattach to c4 and then roll up in the form of vortices at downstream position. The strength of generated vortices in IS flow pattern has increased as compared to those observed in SSB, AR and QSR patterns. It can be seen that the angle of reattachment at (Re, g) = (100, 2.5) is greater than the angle of reattachment at (Re, g) = (200, 1.5). Also the irregularity of shear layer reattachment is more apparent at (Re, g) = (200, 1.5) as compared to (Re, g) = (100, 2.5). The irregular reattachment of flow can also be seen from streamlines behavior (Fig. 19(d)). The stagnant zones can only be seen between the first gap. Bao et al. [25] classified this type of flow behavior as 'non-fully developed vortex street in single row' for flow past six inline square cylinders.

The variation of drag and lift coefficients with time for IS flow is shown in Figs. 13(a)-(d). It can be seen that at (Re, g) = (100, 2.5) the drag coefficient of c1 shows constant behavior

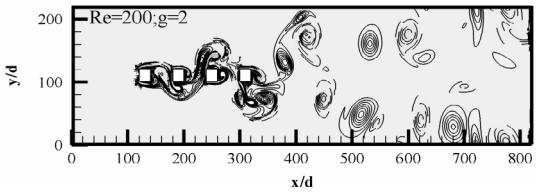

Fig. 14. Vorticity snapshot for CF pattern.

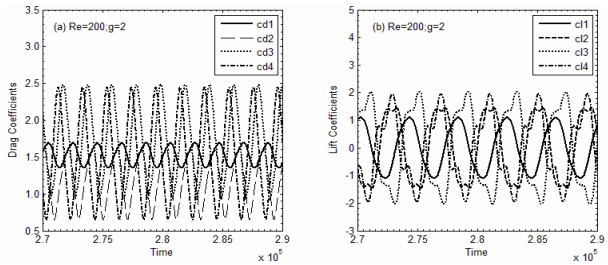

Fig. 15. Temporal histories of drag and lift coefficients for CF pattern.

while the drag coefficients of c2, c3 and c4 have periodic behavior which is due to the merging of shear layers between the gaps (Fig. 13(a)). At (Re, g) = (200, 1.5) it can be seen that the drag and lift coefficients of c1 and c4 show periodic behavior while those of c2 and c3 show irregular behavior which indicates the asymmetrical behavior of flow (Figs. 13(c) and (d)).

5.1.5 Chaotic flow (CF)

Unlike the SSB, AR, QSR and IS flow patterns it can be observed that at (Re, g) = (200, 2) the vortices are generated in the first gap (Fig. 14). But these vortices show complex amalgamation and deformation behavior at downstream position after hitting c2. The generated vortices do not travel in alternate fashion but have irregular movement. This flow behavior is named as Chaotic flow (CF) due to disordered behavior of vortices. The streamlines representation of CF is given in Fig. 19(e). It can be observed that the streamlines do not have waviness instead they have irregular behavior which indicates the chaos in flow. Sewatkar et al. [26] observed such type of flow for six inline square cylinders in the spacing range $6 \leq g \leq 10$ at Re = 100. Similar behavior of flow was observed at (Re, g) = (200, 2.5) and (Re, g) = (200, 7) (Figures not shown). It should be noted that this type of flow was not observed for any chosen spacing value at Re = 100.

The chaotic nature of flow can also be observed from the temporal histories of drag and lift coefficients (Fig. 15). Due to generation of vortices in the first gap the drag as well as lift coefficients of c1 have sinusoidal behavior while the drag coefficients of c2, c3 and c4 have sharp peaks with higher amplitude as compared to other flow patterns. Similarly the lift coefficients also have modulated behavior indicating the distortion of vortices. As the lift coefficients are not sinusoidal, it indicates the presence of secondary frequencies (Cylinder interaction frequencies) in the power spectrum analysis (Fig. 16). The smaller peaks in the power spectrum graphs refer to these cylinder interaction frequencies.

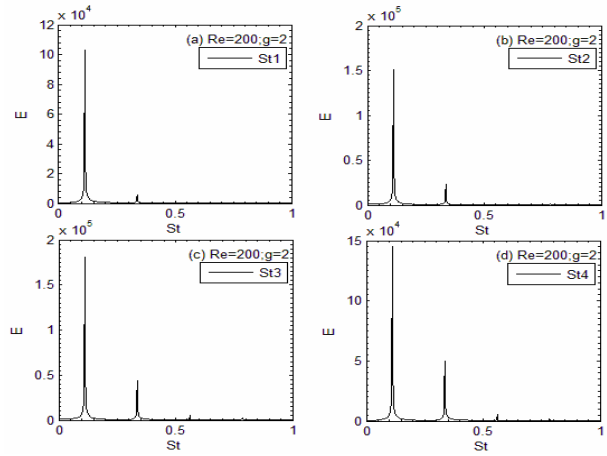

Fig. 16. Power spectrum of lift coefficients for CF pattern.

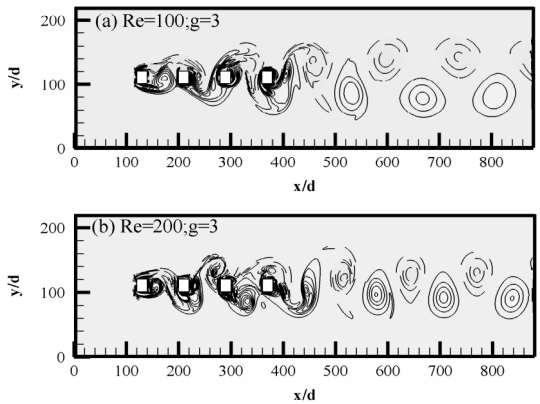

Fig. 17. Vorticity contours visualization for PF pattern.

5.1.6 Periodic flow (PF)

At (Re, g) = (100, 3) and (Re, g) = (200, 3) it can be observed that the vortices are generated in each gap. But due to insufficient space these vortices diminish quickly after hitting the downstream cylinders (Fig. 17). At the downstream position of c4 a Karman vortex street seems to be formed due to alternate generation of vortices. The streamlines also confirm the alternate generation of vortices within the gaps and also at downstream position (Fig. 19(f)). Due to this behavior of flow the time signals of drag as well as lift coefficients of all the cylinders have periodic variation (Fig. 18). This flow pattern is named as Periodic flow (PF). Zdravkovich [1] categorized such type of flow behavior as 'binary vortex street' for the flow past two tandem cylinders due to the fact that both the cylinders shed vortices. Similar flow characteristics were found in the spacing range $3.5 \leq g \leq 7$ at Re =100 and in the spacing range $3.5 \leq g \leq 6$ (Figures not shown). The periodic variation of drag and lift forces indicate the dominancy of vortex shedding frequency in the power spectrum analysis (Figures not shown). For more clear understanding the velocity representation of different observed flow patterns are given in Figs. 20(a)-(f).

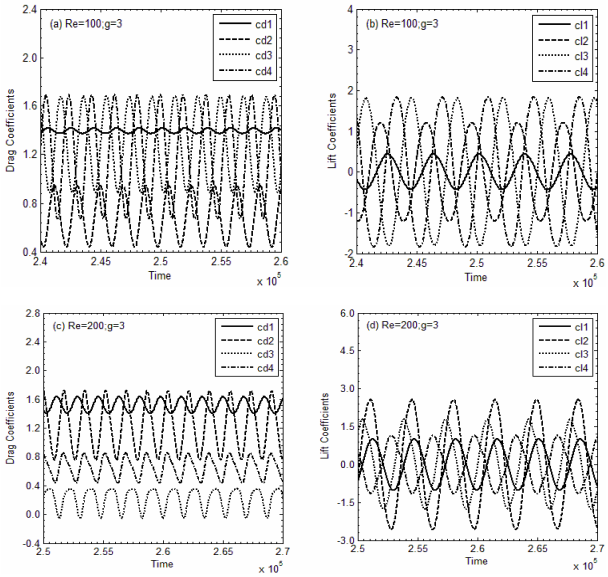

Fig. 18. Temporal variation of drag and lift coefficients for PF pattern.

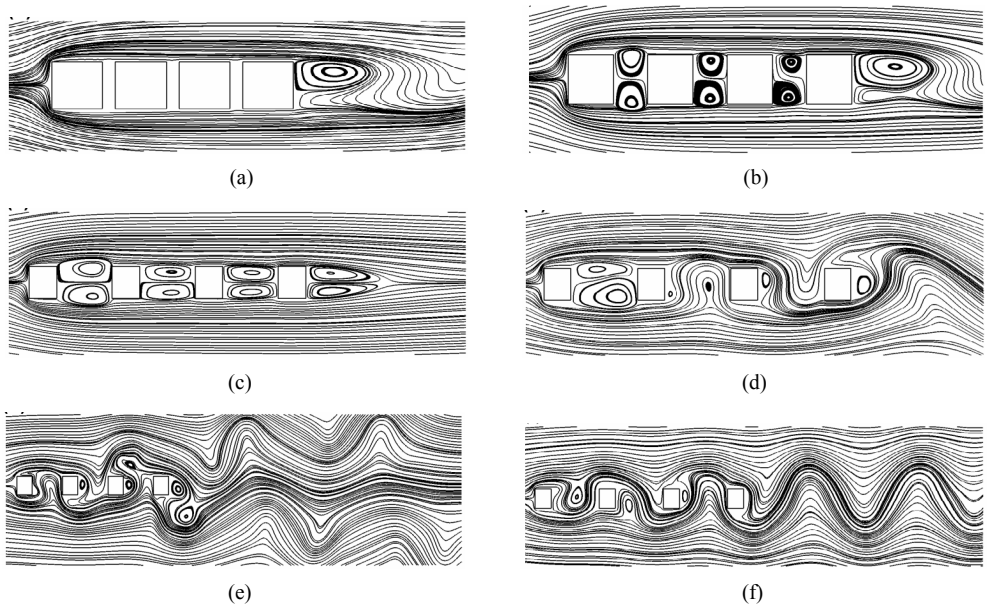

Fig. 19. Streamlines representation of wake patterns: (a) SSB; (b) AR; (c) QSR; (d) IS; (e) CF; (f) PF.

5.1.7 Variation of forces acting on cylinders

Variation of forces acting on cylinders is presented in this section in order to analyze the effect of g on the forces. Fig. 21 presents the effect of g on Cdmean, St, r.m.s values of drag and lift coefficients at Re = 100. The single cylinder values are also presented in the graphs for comparison. It can be seen that the Cdmean1 initially decreases approaching to its minimum value at g = 2.5 while Cdmean2 have negative values up to this spacing value (Fig. 21(a)). This is due to the fact that up to g = 2.5 the vortices are not fully developed in the gaps. The drag force acts as thrust due to pressure difference between rear and front side of c2. As the spacing value approaches to g = 3 both Cdmean1 and Cdmean2 reverse their trends. The Cdmean1 starts increasing behaviour approaching to its maximum value with increment in spacing while Cdeman2 jumps to positive values. This can be supported by the fact that at g = 3 the flow mode changes to PF in which each cylinder starts vortex shedding (Figs. 17(a) and 19(f)). The Cdmean3 and Cdmean4 have similar variation owing different nature from Cmean1 and Cdmean2. Three trends can be observed from their curves. First one is increment in values approaching maxima at g = 3. The second trend is decrement in the values and then both again increase their values. It can also be seen from Cdmean curves that c1 have values closer to that of SC values while other cylinders have sufficiently less values at low gap spacing but gradually these values increase

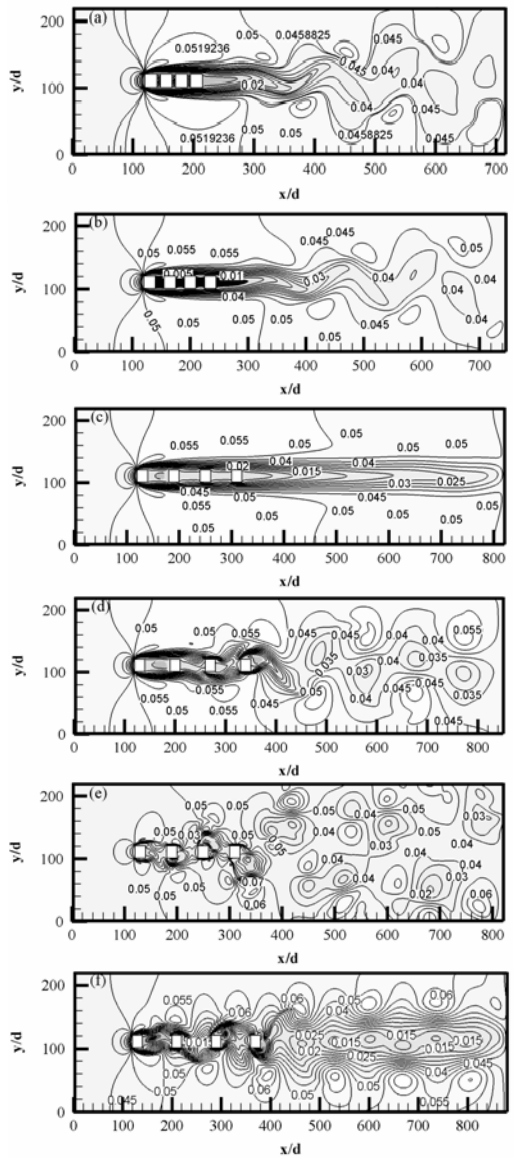

Fig. 20. Velocity representation of wake patterns: (a) SSB; (b) AR; (c) QSR; (d) IS; (e) CF; (f) PF.

approaching to SC values which indicates that with increment in spacing the interference from rear cylinders gradually decreases.

The variation of St of all the cylinders with spacing is shown in Fig. 21(b). A single curve can be seen for St values of all the cylinders up to spacing value g = 4 which indicates that all the cylinders have similar value of St up to g = 4. While at g = 5 c3 and c4 have different value of St than c1 and c2. Also at g = 7 c4 have different value of St than other three cylinders. This is due to the effect of cylinder interaction frequencies. Further it can be seen that the value of St is smaller than SC at low spacing values. It decreases initially approaching to minimum value at g = 2 where the QSR flow pattern was observed (Fig. 10). According to Xu and Zhou [11] vortices do not generate between the gaps at small spacing values

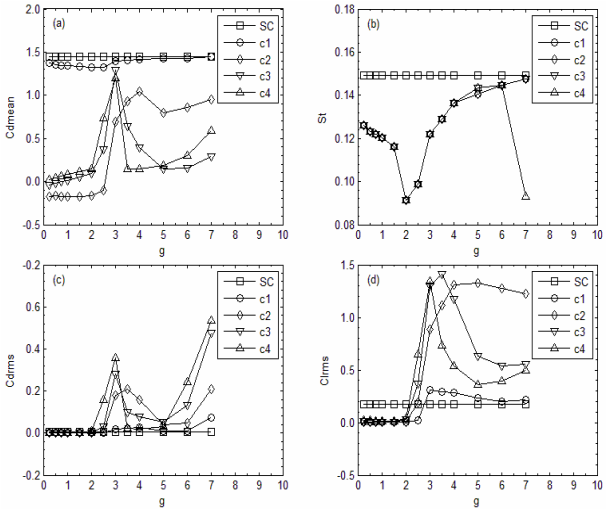

Fig. 21. Variation of (a) Cdmean; (b) St; (c) Cdrms; (d) Clrms with spacing at Re = 100.

which results in decrease in St. After g = 2 St starts increasing and have a jump at g = 3 approaching towards SC values. At g = 7 the St of c1, c2 and c3 comes sufficiently close to SC values. This increment in values of St is due to the fact that after g = 2 the vortices start to generate between the gaps. While at g = 7 vortices are fully generated in each gap.

The Cdrms curves of all the cylinders have similar variation with spacing (Fig. 21(c)). Initially these curves have constant behavior having almost similar values to SC. After that these curves increase to higher values than SC, then decrease approaching towards SC values in the spacing range $3.5 \leq g \leq 5$. After that these curves again show increasing behavior.

The Clrms of all the cylinders have less values as compared to SC in the spacing range $0.25 \leq g \leq 2.5$ (Fig. 21(d)). When the flow mode changes to PF pattern, the Clrms of c1, c3 and c4 show similar variation with increment in spacing. They have increasing behavior in the spacing range $3 \leq g \leq 4$, decreasing behavior in the spacing range $4 \leq g \leq 6$ and then again have increasing behavior after that.

The effect of g on Cdmean, St, Cdrms and Clrms at Re = 200 is presented in Fig. 22. It can be observed from Figs. 21 and 22 that the Cdmean1 at Re = 200 is generally higher than Cdeman1 at Re = 100 at a specific spacing value. This indicates that at Re = 200 c1 experiences higher drag forces as compared to those at Re = 100. Similar trend can be observed in SC values at Re = 200 and Re = 100. Further it can be observed that the Cdmean1 slightly decreases in the spacing range $0.25 \leq g \leq 1.5$ (Fig. 22(a)). But when the spacing value approaches to g = 2 it jumps to its maximum value. Similarly Cdmean2 changes from negative to positive at g = 2. While Cdmean3 and Cdmean4 both increase upto g = 2.5 aproaching to their maximum values. It sholud be noted that at g = 2 and 2.5 the CF pattern was observed. It can be seen that at these spacing values some of the values of Cdmean are higher than those of SC. This is due to deformation of vortices. At g = 2.5

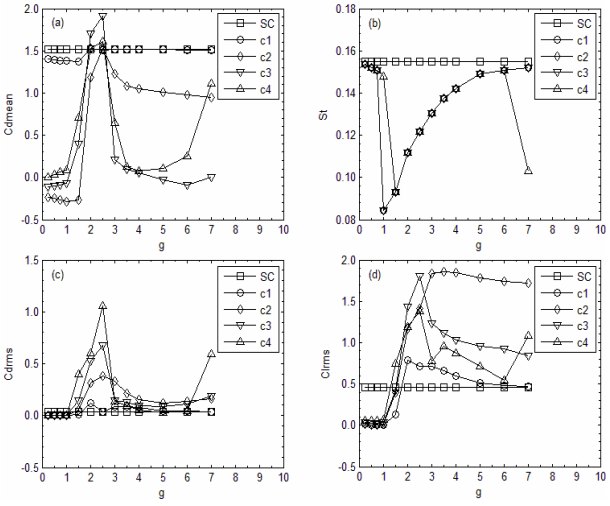

Fig. 22. Variation of (a) Cdmean; (b) St; (c) Cdrms; (d) Clrms with spacing at Re = 200.

Cdmean3 attains highest value 1.9135 observed in this study. According to Zdravkovich [1] this is due to the effect of turbulance in the boundary layer which results in increasing the forces acting on downstream cylinders than the upstream ones. Also it can be seen that at g = 0.25 the downstream cylinders c1, c2 and c3 all have negative value of Cdmean.

The St of all the cylinders decreases in the spacing range $0.25 \leq g \leq 1.5$ approaching to minimum value (Fig. 22(b)). But when the flow mode changes to CF pattern it increases approaching to SC values. At g = 1 and 7 the St of c4 is different from other cylinders due to the effect of cylinder interaction frequencies. Further it can be observed that the Cdrms2 and Cdrms3 curves have similar variation with spacing increment (Fig. 22(c)). Initially both have constant behavior then increase in the spacing range $1.5 \leq g \leq 2.5$. After that both decrease in the range $3 \leq g \leq 5$ and then again have increasing behavior. The Clrms of all cylinders is less than that of SC in the spacing range $0.25 \leq g \leq 1$due to the fact that the vortices are not generated in the gaps due to narrow gaps. Also Clrms2 and Clrms3 exhibit similar trend with spacing (Fig. 22(d)). Both initially decrease to minimum value, then increase approching maximum value and after that once again have decreasing behavior. While the Clrms1 and Clrms4 have similar variation to each other. Further it can be observed that the Clrms values are greater than the corresponding Cdrms values at both Re = 100 and 200 (Figs. 21(c), (d) and 22(c), (d)).

6. Conclusions

Numerical calculations were performed in order to investigate the effects of spacing on the variation of wake patterns and force coefficients of the flow past four square bodies aligned inline. A 2D-numerical code was developed at two different Reynolds numbers 100 and 200 using the lattice Boltzmann method (MRT-LBM). The code was first validated for the flow past single and two tandem bodies by comparing the results to those available in literature. The results were found to be in good agreement to the available data. After validation the calculations were further performed for the flow past four square bodies aligned inline. Important findings of this study are given below:

Six different wake patterns were found in this study. These are: (a) Single slender body, (b) Alternate reattachment, (c) Quasi steady reattachment, (d) Intermittent shedding, (e) Chaotic flow and (f) Periodic flow.

At some moderate spacing values the flow mode was completely different at Re = 100 and 200. For example, the Quasi Steady reattachment pattern was found at Re = 100 only while the Chaotic flow was observed at Re = 200 only. Generally strengthened vortices were found at Re = 200 as compared to those at Re = 100.

At Re = 100 the spacing value g = 3 was found to be critical while at Re = 200 the spacing value g = 2 was found to be critical due to abrupt changes in flow behavior and force coefficients.

At Re = 100 the middle two cylinders have negative values of average drag coefficient (Cdmean) in the spacing range $0.25 \leq g \leq 0.75$ while at Re = 200 the negative values were found in the spacing range $0.25 \leq g \leq 1$.

The highest value of Cdmean was found in the Chaotic Flow pattern while the lowest value was found in the Alternate Reattachment flow pattern.

Generally all the cylinders have similar values of Strouhal number (St) but at some spacing values the downstream cylinders have different values of St than the upstream ones.

The root mean square values of lift coefficient were found to be greater than the corresponding root mean square values of drag coefficients.

Nomenclature

cd	: Drag coefficient
cd1	: Drag coefficient of upstream cylinder
cd2	: Drag coefficient of second cylinder
cd3	: Drag coefficient of third cylinder
cd4	: Drag coefficient of downstream cylinder
cl	: Lift coefficient
cl1	: Lift coefficient of upstream cylinder
cl2	: Lift coefficient of second cylinder
cl3	: Lift coefficient of third cylinder
cl4	: Lift coefficient of downstream cylinder
c1	: Upstream cylinder
c2	: Second cylinder
c3	: Third cylinder
c4	: Downstream cylinder
Cdmean	: Mean drag coefficient
Cdmean1	: Mean drag coefficient of upstream cylinder
Cdmean2	: Mean drag coefficient of second cylinder
Cdmean3	: Mean drag coefficient of third cylinder

Cdmean4 : Mean drag coefficient of downstream cylinder
Cdrms : Root-mean-square value of drag coefficient
Cdrms1 : Root-mean-square value of drag coefficient of upstream cylinder
Cdrms2 : Root-mean-square value of drag coefficient of second cylinder
Cdrms3 : Root-mean-square value of drag coefficient of third cylinder
Cdrms4 : Root-mean-square value of drag coefficient of downstream cylinder
Clrms : Root-mean-square value of lift coefficient
Clrms1 : Root-mean-square value of lift coefficient of upstream cylinder
Clrms2 : Root-mean-square value of lift coefficient of second cylinder
Clrms3 : Root-mean-square value of lift coefficient of third cylinder
Clrms4 : Root-mean-square value of lift coefficient of downstream cylinder
d : Size of the cylinder
F_d : In-line force component
F_l : Transverse force component
f_s : Vortex shedding frequency
g : Gap spacing
H : Height of the computational domain
K : Shear parameter
L : Length of the computational domain
Ld : Downstream position
Lu : Upstream position
Re : Reynolds number
s : Surface-to-surface distance between cylinders
St : Strouhal number
St1 : Strouhal number of upstream cylinder
St2 : Strouhal number of second cylinder
St3 : Strouhal number of third cylinder
St1 : Strouhal number of downstream cylinder
U_∞ : Uniform inflow velocity
U_r : Mean free stream velocity

Greek symbols

ν : Kinematic viscosity
ρ : Fluid density

References

[1] M. M. Zdravkovich, The effects of interference between circular cylinders in cross flow, *Journal of Fluids and Structures,* 1 (1987) 239-261.
[2] W. C. L. Shih, C. Wang, D. Coles and A. Roshko, Experiments on flow past rough circular cylinders at large Reynolds numbers, *Journal of Wind Engineering and Industrial Aerodynamics,* 49 (1993) 351-368.
[3] H. J. Niemann and N. Holscher, A review of recent experiments on the flow past circular cylinders, *Journal of Wind Engineering and Industrial Aerodynamics,* 33 (1990) 197-209.
[4] S. Manzoor, J. Khawar and N. A. Sheikh, Vortex-induced vibrations of a square cylinder with damped free-end conditions, *Advances in Mechanical Engineering* (2013) 1-12.
[5] R. Franke, W. Rodi and B. Schonung, Numerical calculation of laminar vortex-shedding flow past cylinders, *Journal of Wind Engineering and Industrial Aerodynamics,* 35 (1990) 237-257.
[6] A. k. Saha, k. Muralidhar and G. Biswas, Transition and chaos in two-dimensional flow past a square cylinder, *Journal of Engineering Mechanics,* 126 (2000) 523-532.
[7] M. Cheng, D. S. Whyte and J. Lou, Numerical simulation of flow around a square cylinder in uniform-shear flow, *Journal of Fluids and Structures,* 23 (2007) 207-226.
[8] S. Dutta, P. K. Panigrahi and K. Muralidhar, Experimental investigation of flow past a Square cylinder at an angle of incidence, *Journal of Engineering Mechanics,* 134 (2008) 788-803.
[9] A. Sohankar, L. Davidson and C. Norberg, Numerical simulation of unsteady flow around a square two-dimensional cylinder, *Twelfth Australian Fluid Mechanics Conference,* The University of Sydney, Australia (1995) 517-520.
[10] N. Mahir, Three-dimensional flow around a square cylinder near a wall, *Ocean Engineering,* 36 (2009) 357-367.
[11] G. Xu and Y. Zhou, Strouhal numbers in the wake of two inline cylinders, *Experiments in Fluids,* 37 (2004) 248-256.
[12] M. K. Kim, D. K. Kim, S. H. Yoon and D. H. Lee, Measurements of the flow fields around two square cylinders in a tandem arrangement, *Journal of Mechanical Science and Technology,* 22 (2008) 397-407.
[13] A. Lankadasu and S. Vengadesan, Interference effect of two equal-sized square cylinders in tandem arrangement: With planar shear flow, *International Journal for Numerical Methods in Fluids,* 57 (2007) 1005-1021.
[14] A. Sohankar, A numerical investigation of the flow over a pair of identical square cylinders in a tandem arrangement, *International Journal for Numerical Methods in Fluids*, 70 (2011) 1244-1257.
[15] P. P. Patil and S. Tiwari, Numerical investigation of laminar unsteady wakes behind two inline square cylinders confined in a channel, *Engineering Applications of Computational Fluid Mechanics*, 3 (2009) 369-385.
[16] J. R. Meneghini, F. Saltara, C. L. R. Siqueira and J. A. Ferrari Jr., Numerical simulation of flow interference between two circular cylinders in tandem and side-by-side arrangements, *Journal of Fluids and Structures,* 15 (2001) 327-350.
[17] D. B. Ghadiri, M. H. Sarvghad and J. H. Houri, Numerical simulation of flow over two circular cylinders in tandem arrangement, *Journal of Hydrodynamics,* 23 (2011) 114-126.
[18] A. Sohankar, A LES study of the flow interference between tandem square cylinder pairs, *Theoratical and Computational Fluid Dynamics,* 28 (2014) 531-548.
[19] O. Inoue, M. Mori and N. Hatakeyama, Aeolian tones radi-

ated from flow past two square cylinders in tandem, *Physics of Fluids,* 18 (2006) 1-15.

[20] C. K. Vikram, Y. T. Krishne, H. V. Ravindra and C. J. Gangadara, Manu, Numerical simulation of two dimensional unsteady flow past two square cylinders, *International Journal of Technology And Engineering System,* 2 (2011) 355-360.

[21] T. Igarashi and K. Suzuki, Characteristics of the flow around three circular cylinders arranged in line, *Bulletin of JSME,* 27 (1984) 2397-2404.

[22] A. B. Harichandan and A. Roy, Numerical investigation of low Reynolds number flow past two and three circular cylinders using unstructured grid CFR scheme, *International Journal of Heat and Fluid Flow,* 31 (2010) 154-171.

[23] A. R. Vasel-Be-Hagh, D. Ting and R. Carriveau, Correlating flow pattern with force coefficients in air flow past a tandem unit of three circular cylinders, *International Journal of Fluid Mechanics Research,* 40 (2013) 235-253.

[24] S. U. Islam, W. S. Abbasi, H. Rahman and R. Naheed, Numerical investigation of wake modes for flow past three tandem cylinders using the multi-relaxation-time lattice Boltzmann method for different gap spacings, *Journal of the Brazilian Society of Mechanical Sciences and Engineering*, DOI 10.1007/s40430-014-0282-4.

[25] Y. Bao, Q. Wu and D. Zhou, Numerical investigation of flow around an inline square cylinder array with different spacing ratios, *Computers & Fluids,* 55 (2012) 118-131.

[26] C. M. Sewatkar, R. Patel, A. Sharma and A. Agrawal, Flow around six in-line square cylinders, *Journal of Fluid Mechanics,* 710 (2012) 195-233.

[27] S. Chen and G. Doolen, Lattice Boltzmann method for fluid flows, *Annual Review of Fluid Mechanics*, 30 (1998) 329-364.

[28] P. Lallemand and L. S. Luo, Theory of the lattice Boltzmann method: Acoustic and thermal properties in two and three dimensions, *Physical Review E*, 68 (3) (2003) 036706.

[29] G. M. Kremer, *An introduction to the Boltzmann equation and transport processes in gases*, Springer (2010).

[30] Z. Guo, H. Liu, L. Luo and K. Xu, Comparative study of the LBE and GKS methods for 2D near incompressible laminar flows, *Journal of Computational Physics,* 227 (2008) 4955-4976.

[31] D. Yu, M. Renwei, L. S. Luo and S. Wei, Viscous flow computations with the method of lattice Boltzmann equation, *Progress in Aerospace Sciences,* 39 (2003) 329-367.

[32] A. Okajima, Strouhal numbers of rectangular cylinders, *Journal of Fluid Mechanics,* 123 (1982) 379-398.

[33] C. Norberg, Flow around rectangular cylinders: Pressure forces and wake frequencies, *Journal of Wind Engineering and Industrial Aerodynamics,* 49 (1993) 187-196.

[34] A. S. Abograis and A. E. Alshayji, Reduction of fluid forces on a square cylinder in a laminar flow using passive control methods, *COMSOL Conference*, Boston, USA (2013).

[35] W. S. Abbasi, S. Ul. Islam, S. C. Saha, Y. T. Gu and C. Y. Zhou, Effect of Reynolds numbers on flow past four square cylinders in an in-line square configuration for different gap spacings, *Journal of Mechanical Science and Technology*, 28 (2) (2014) 539-552.

[36] H. R. Kim, M. Ha, H. S. Yoon and S. W. Son, Dynamic behavior of a droplet on a moving wall, *Journal of Mechanical Science and Technology*, 28 (5) (2014) 1709-1720.

[37] J. Bang and W. Yoon, Stochastic analysis of a collection process of submission particles on a single fiber accounting for the changes in flow field due to particle collection, *Journal of Mechanical Science and Technology*, 28 (9) (2014) 3719-3732.

[38] N. Jeong, Rarefied gas flow simulation with TMAC in the slip and the transition flow regime using the lattice Boltzmann method, *Journal of Mechanical Science and Technology*, 28 (11) (2014) 4705-4715.

[39] S. Ul. Islam, H. Rahman, W. S. Abbasi, U. Noreen and A. Khan, Suppression of fluid force on flow past a square cylinder with a detached flat plate at low Reynolds number for various spacing ratios, *Journal of Mechanical Science and Technology*, 28 (12) (2014) 4969-4978.

[40] M. Jourabian and M. Farhadi, Melting of nanoparticles-enhanced phase change material (NEPCM) in vertical semi-circle enclosure: numerical study, *Journal of Mechanical Science and Technology*, 29 (9) (2015) 3819-3830.

[41] S. Ul. Islam, C. Y. Zhou, A. Shah and P. Xie, Numerical simulation of flow past rectangular cylinders with different aspect ratios using the incompressible lattice Boltzmann method, *Journal of Mechanical Science and Technology*, 26 (4) (2012) 1027-1041.

Shams-ul-Islam is currently a assistant professor in Mathematics Department COMSATS Institute of Information, Technology, Islamabad. He received his Ph.D. in 2010. His research interests include, fluid structure interaction, drag reduction of bluff body and heat and mass transfer.